Photophysics and Binding Constant Determination of the Homodimeric Dye BOBO-3 and DNA Oligonucleotides

Maria J. Ruedas-Rama, Angel Orte, Luis Crovetto, Eva M. Talavera, and Jose M. Alvarez-Pez*

Department of Physical Chemistry, Faculty of Pharmacy, University of Granada, Campus Cartuja, 18071, Granada, Spain

Received: October 14, 2009; Revised Manuscript Received: November 17, 2009

The interactions between single- and double-stranded DNA and the trimethine cyanine homodimer dye, BOBO-3 (1,1′-(4,4,7,7-tetramethyl-4,7-diazaundecamethylene)-bis-4-[3-methyl-2,3-dihydro-(benzo-1,3-thiazole)-2-methylidene]pyridinium tetraiodide), have been investigated in detail using absorption and steady-state and time-resolved fluorescence spectroscopy. The dye interacts with both single-stranded and double-stranded DNA, under a variety of conditions, with changes in its spectral characteristics. Our results indicated that the complex formed between BOBO-3 dye and DNA oligonucleotides could not be explained with a simple, single intercalation mechanism; therefore, different modes of interaction were proposed. By using time-resolved fluorescence methodology and in-depth analysis of the fluorescence decay traces, we obtained the contribution of the different forms of BOBO-3: free in solution, a low affinity, electrostatically driven interaction with DNA, and a full bis-intercalation mechanism within the DNA double helix. With this information, we applied the McGhee−Von Hippel theory for two overlapping, noncooperative binding modes to obtain equilibrium binding constants and the number of sites occupied for each binding mode. Binding constants for dye/dsDNA complexes in complete bis-intercalation and externally bound were $(8.8 \pm 1.1) \times 10^5$ and $(2.6 \pm 0.3) \times 10^5$ M^{-1}, respectively. The corresponding recovered number of base pairs covered were 5.9 ± 0.2 and 3.5 ± 0.5 sites for each mode.

Introduction

Cyanine dyes are a valuable family of fluorophores. On the basis of the stability of complexes between double-stranded DNA (dsDNA) and the bis-intercalator ethidium homodimer (EtD),[1] Rye et al. have synthesized dimeric cyanine dyes with affinity for ds-DNA higher even than that of EtD, due to the four positive charges in their molecular structures.[2,3] The two first dyes reported were the oxazole yellow homodimer, YOYO-1, and the thiazole yellow homodimer, TOTO-1.[4] They are largely used in nucleic acid staining, because they reduce the hazards in handling relatively concentrated solutions of the conventional intercalator ethidium bromide, EtBr. The members of this family of dyes show large fluorescence enhancements when bound to dsDNA, and the complexes remain stable during electrophoresis. However, there is still a lack of understanding of their photophysical properties and binding affinities.

The studies to date on dsDNA binding features of dimeric cyanine dyes have been focused on both YOYO-1 and TOTO-1. It has been proposed that both dyes exhibit two distinct binding modes to dsDNA.[5,6] At mixing ratios dye:DNA base up to 0.125 for YOYO-1, the predominant mode of binding is bis-intercalation, with the long axis of the YO chromophore oriented parallel to the long axis of the base pair pocket. For dye:base pair ratios higher than 0.125, a secondary binding mode to the DNA begins to contribute noticeably.[5] The main aspects about this behavior were also observed for TOTO-1 homodimer,[7] although the interaction with dsDNA and single-stranded DNA (ssDNA) are of similar high affinity.[8] An external binding mode, where the dipole of the dye molecule is aligned with the DNA grooves, has been suggested from fluorescence polarization measurements.[9] Nevertheless, although these latest conclusions were well established, no binding constant values were recovered.

In previous work, we proposed a DNA hybridization detection methodology in homogeneous media based on fluorescence resonance energy transfer (FRET) between xanthenic dyes and dsDNA intercalating fluorophores.[10] We have recently sought better energy transfer acceptors for this approach and considered the features of dimeric cyanine dye BOBO-3. Nevertheless, little is known about the binding modes and specificity between the dimeric cyanine dye BOBO-3 and both ssDNA and dsDNA. We are therefore interested in studying in depth the nature and magnitude of these interactions for a better understanding of the mechanisms of FRET between the intercalating dye and xanthenic derivatives.

Intercalative binding to DNA is a type of noncooperative binding and is well described by the McGhee−Von Hippel theory.[11] Nevertheless, the resulting equations cannot be solved by steady-state fluorescence analysis if the complex dye−DNA displays two distinct binding modes, although it could be a valid approximation at very low dye/bp ratios.[12] Likewise, the indirect method carried out with competing ligands and employed for calculating the association constants of dimeric intercalating drugs, such as EtD, suffer from the same problems.[13] The steady-state fluorescence methodologies employed to solve the McGhee−Von Hippel theory were based on rough assumptions that research on time-resolved fluorescence has proven to be unsuitable.[14,15]

As it is known, the quantitative resolution of discrete fluorescence lifetimes from a fluorescence decay curve may

* Corresponding author. E-mail: jalvarez@ugr.es. Tel: +34 958 243831. Fax: +34 958 244090.

10.1021/jp909863c
Published on Web 12/08/2009

reflect different fluorophores or molecular interactions of the probe within a particular microsurrounding of a target macromolecule.[16] Fluorescence lifetime measurements for some acridine dyes complexed to DNA have been reported, exhibiting either bi- or triexponential emission decay kinetics reflecting different modes of binding. For instance, fluorescence decay traces from aqueous EtBr−dsDNA solutions showed three lifetimes.[14,17] These three lifetimes were assigned to the three different populations of EtBr involving distinct environments in the aqueous EtBr−dsDNA solutions, namely a short-lived component corresponding to the remaining free EtBr, a long-lived component associated with the excited-state lifetime of the intercalated EtBr, and an intermediate-lived component between the free and intercalated values which was associated with the lifetime of EtBr binding at the external secondary sites. The global analysis of the fluorescence decay surface from EtBr−dsDNA solutions at different dye/bp ratios led to the constant values and site numbers of the intercalative and secondary binding.[17] The time-resolved method has also been used for determining the ss- to ds-DNA ratio from the dye−DNA complexes.[18]

The present study makes use of steady-state and time-resolved fluorescence methodologies to compare the interaction of BOBO-3 with ssDNA and dsDNA under a variety of conditions and to determine the binding modes and binding constant of each mode. We have used the time-correlated single photon counting method, TCSPC, for obtaining accurate fluorescence decay data which allow the resolution of all decay time components of buffered BOBO-3/DNA solutions. Moreover, the normalized weighting coefficients from lifetimes provided the fractional excited-state population of fluorophores into each microsurrounding. Thus, with this simple approach we can quantify, by a direct method, the concentrations of free, bis-intercalated, and external bound BOBO-3, and apply the McGhee−von Hippel expression to separately obtain the binding constants and the number of binding sites.

Materials and Methods

Reagents. All experiments were performed using chemicals of analytical-reagent grade and Milli-Q water. Buffer salt of Tris, sodium chloride, and EDTA were obtained from Sigma-Aldrich. The pH of solutions and buffers was adjusted using diluted NaOH (Aldrich, Spain) and HCl (Aldrich, Spain) (spectroscopic grade quality) dissolved in Milli-Q water. All of the chemicals were used as received without further purification, and the stock solutions were protected from sunlight and kept at 4 °C in a refrigerator. In all staining procedures, BOBO-3 iodide stock solution (Invitrogen, Carlsbad, CA) was diluted fresh in 1 mM EDTA, 100 mM NaCl, and 10 mM Tris buffer solution at pH 7.5. In intercalation experiments BOBO-3 was added to the DNA solutions and incubated for 10 min in the dark at 25 °C.

Oligonucleotides. The chemically synthesized oligonucleotides sequences (5′-CTA CTA CAA CTG GAA GAC CGG GAA GTC CGA GAA GTG CAT CTT CTG C-3′, 5′-GCA GAA GAT GCA CTT CTC GGA CTT CCC GGT CTT CCA GTT GTA GTA G-3′, 5′-CTA CTA CAA CTG GAA-3′, and 5′-TTC CAG TTG TAG TAG-3′) were obtained from IBA Technologies (Germany). The DNA was purified by double HPLC and dissolved in 1 mM EDTA, 100 mM NaCl, and 10 mM Tris buffer at pH 7.5. The base sequences correspond to a gene fragment of *Halomonas Ventosae* bacteria (gene *narH* Al12). All subsequent dilutions were also prepared in the same buffer. The ssDNA sequences were annealed with their corresponding complementary strand to form the respective dsDNA. The hybridization was performed by heating at 95 °C for 5 min and slowly cooling to room temperature. The stock ssDNA concentration was verified by absorption measurements at 260 nm. Oligonucleotides solutions used in the measurements of spectral properties ranged 25−500 nM in dsDNA or ssDNA.

Instruments. Absorption spectra were recorded with a Perkin-Elmer Lambda 650 UV/vis spectrophotometer with a Peltier temperature-controlled cell holder. All measurements were made at 25 °C, using 5 × 10 mm cuvettes. Steady-state fluorescence emission spectra were collected on a JASCO FP-6500 spectrofluorometer equipped with a 450 W xenon lamp for excitation, with temperature controller ETC-273T at 25 °C.

Fluorescence decay traces of BOBO-3 in solution and interacting with single-stranded and double-stranded DNA of different lengths were recorded in the time-correlated single photon counting (TCSPC) mode using the FluoTime 200 fluorometer (PicoQuant, GmbH). The excitation was by a 485-nm pulsed laser (LDH-P-C-485 PicoQuant, GmbH) with a 20 MHz repetition rate. The full width at half-maximum of the laser pulse was ∼80 ps. The fluorescence was collected after crossing through a polarizer set at the magic angle and a 2 nm bandwidth monochromator. Fluorescence decay histograms were collected using a TimeHarp200 board, with a time increment per channel of 36 ps, at the emission wavelengths of 590, 600, 610, and 620 nm. Histograms of the instrument response functions (using LUDOX scatterer) and sample decays were recorded until they typically reached 2×10^4 counts in the peak channel.

Methods of Analysis. Apparent quantum yield values from steady-state fluorescence measurements were calculated using eq 1:

$$\Phi = \Phi_R \frac{I}{I_R} \frac{OD_R}{OD} \frac{n^2}{n_R^2} \quad (1)$$

where Φ is the quantum yield, I is the integrated intensity, OD is the optical density, and n is the refractive index. The subscript R refers to a reference fluorophore of known quantum yield. In the cases of the determination of quantum yield of BOBO-3 free in solution, BOBO-3 interaction with ssDNA, and intercalation into dsDNA at different BOBO-3/bp ratios, rhodamine B in ethanol was used as reference ($\Phi = 0.31$).[19]

Time-resolved fluorescence decay traces were analyzed by using FluoFit 4.4 package (Picoquant GmbH). The experimental decay traces were fitted to multiexponential functions via a Levenberg−Marquard algorithm-based nonlinear least-squares error minimization deconvolution method. Global fits of the four different emission wavelengths collected, 590, 600, 610, and 620 nm, were performed by making the lifetimes τ_i as shared global adjustable parameters, and the pre-exponential factors were locally adjustable. Usually, up to three different exponential terms were used to fit the experimental decay traces. In the fitting, the shortest lifetime was kept fixed to the value of the lifetime of BOBO-3 in solution. The quality of fittings was judged by the reduced chi-squared method, χ^2, the weighted residuals, and the correlation functions. The latter two were checked for random distributions.

In order to calculate the contribution of BOBO-3 participation in the different interactions, the values of the pre-exponential factors obtained in the decay trace fit were converted into mole fractions, taking into account the differential excitation rates of the distinct dye species at the laser excitation wavelength, as

well as the different contributions at each emission wavelength of the three species (see Supporting Information and Table S1 for details).

Once the fraction of BOBO-3 bound in each mode to DNA is known by the procedure described above, it is possible to apply the McGhee−Von Hippel theory in order to estimate the binding affinity constants and the number of binding sites occupied for each mode. The procedure is based on a nonlinear regression model, via minimization of weighted residuals, and it is detailed in Supporting Information. The goal is to numerically solve and globally fit McGhee−Von Hippel equations to our experimental data for each different binding mode j to recover their respective binding constant K_j and the number of base pairs covered in each mode n_j:

$$r_j = \mathrm{DNA_{bp}} K_j \frac{[1 - \sum_j n_j r_j]^{n_j}}{[1 - \sum_j (n_j - 1) r_j]^{n_j - 1}} (r_{\mathrm{tot}} - \sum_j r_j) \quad (2)$$

where r_j is the concentration of complexed dye per dsDNA base pair in each mode, and r_{tot} is the total concentration of fluorophore added per base pair, and $\mathrm{DNA_{bp}}$ is the total molar concentration of base pairs. These equations are not explicit so it is not possible to apply direct nonlinear regression methods; however, the equations can be solved numerically based on the algorithm proposed by Gaugain et al.[13] Therefore, the global fitting algorithm for two different binding modes is in brief as follows: (1) the experimental concentrations of bound BOBO-3 in each mode and BOBO-3 in solution are known by the time-resolved fluorescence analysis, so by using the known base pair concentration they can be expressed in terms of r_1, r_2 and r_{tot}; (2) from the initial guesses of K_1, K_2, n_1 and n_2, the curves r_1 vs r_{tot} and r_2 vs r_{tot} are numerically obtained; (3) the residuals can be then estimated and weighted by the standard deviation in the determination of each data point (from repetitions); (4) the adjustable parameters are then varied to minimize the sum of the squared weighted residuals (for both binding modes simultaneously). It is important to note that the r_j values depend on the total dsDNA concentration; therefore, when there are experimental points taken at different total nucleic acid concentration several r_j vs r_{tot} curves must be obtained and compared to the corresponding results at the appropriate DNA concentration. The fitting process is feasible by embedding the numerical simulation within the least-squares minimization method and was coded using MathCad 14.0 (PTC, Needham, MA). For further details, see Supporting Information and Figure S1.

Results

Absorption Spectroscopy. Figure 1A shows the absorption spectra of BOBO-3 under different experimental conditions. In the visible region free BOBO-3 in solution presents a band with absorption maximum at 534 nm and a shoulder around 560 nm. In the presence of large amounts of dsDNA the absorption band is red-shifted and the maximum is at 571 nm, having an almost Gaussian shape. When an excess of BOBO-3 is present, an additional shoulder appears at lower wavelengths and the maximum is slightly blue-shifted. Moreover, we noted that BOBO-3 also interacts with ssDNA, showing an absorption maximum shifted to 567 nm and a shoulder, similar to that in the case of excess of intercalators in dsDNA. These spectral features were similar regardless of the oligonucleotide length,

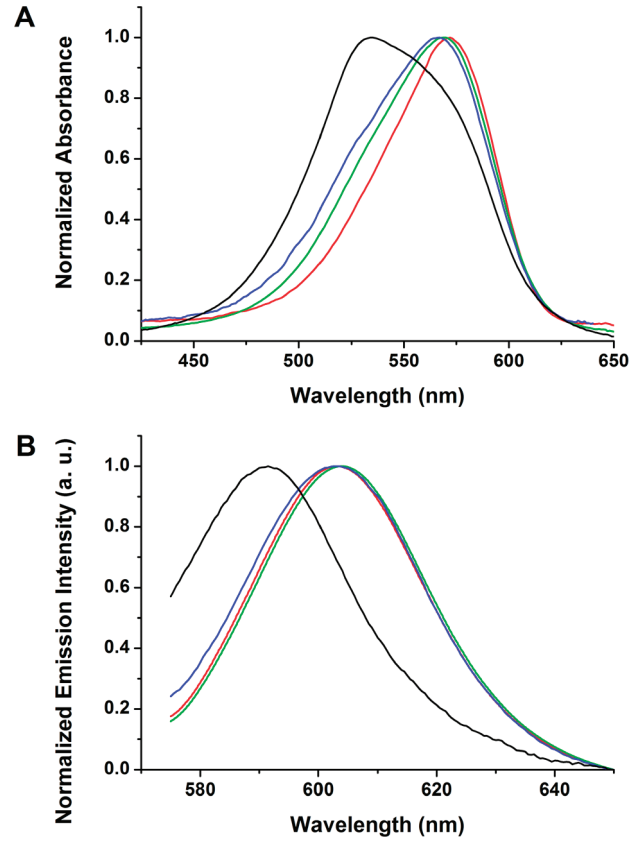

Figure 1. Normalized absorption spectra (A) and emission spectra (λ_{ex} = 571 nm) (B) of BOBO-3 free in solution (black), BOBO-3/46 nucleotides-ssDNA in a ratio 1:1 (blue), BOBO-3/dsDNA (46 bp) in a ratio 1:100 (red), and BOBO-3/dsDNA (46 bp) in a ratio 5:1 (green). Note the fluorescence emission of BOBO-3 in solution is much weaker than interacting with DNA. The normalization factors were according to the quantum yields given in Table 1.

in our tested 15- and 46-nucleotide ssDNA and the corresponding double-stranded DNA of the same lengths.

Steady-State Fluorescence Spectroscopy. The dye in solution showed a low emission intensity, with a weak band at 590 nm, whereas an enhancement of the fluorescence was detected upon addition of either ssDNA or dsDNA, and a concomitant red-shift of the emission maximum to 602 nm (λ_{ex} = 571 nm) (Figure 1B). We first studied the fluorescence emission enhancement characteristics of BOBO-3 upon binding to dsDNA (15 and 46 bp). We then recorded steady-state emission spectra in the range of dsDNA concentration between 5×10^{-8} and 5×10^{-7} M in hybridization buffer at pH 7.5, and increasing concentrations of BOBO-3. Figure 2A shows the fluorescence emission intensity at 602 nm versus the ratio of BOBO-3 over base pair concentrations for 46 bp dsDNA (λ_{ex} = 571 nm). A linear increase was detected at low dye concentrations until a gradual plateau was reached, and finally the fluorescence signal even started to decrease. Typically, the intersection point between the increasing slope and the plateau region has been considered to provide a rough estimate of the saturation, or number of binding sites per nucleotide bases,[8] a situation in which most of the binding sites are covered. The fluorescence decrease at high excess of BOBO-3 can be attributed to a self-quenching or homo-energy transfer between molecules of dye in close proximity. As can be seen in Figure 2, the saturation number estimated through this method clearly showed a dependence on the total dsDNA concentration present. Higher dsDNA concentrations showed saturation at a lower number of intercalating dye molecules per base pair. This demonstrates

TABLE 1: Summary of Some Spectral Characteristic of BOBO-3 in Solution and Interacting with Different Types of DNA

	BOBO-3 in solution	ssDNA (15b)/BOBO-3	ssDNA (46b)/BOBO-3	dsDNA (15 bp)/BOBO-3	dsDNA (46 bp)/BOBO-3
maximum absorbance (nm)	534	566	567	571	571
maximum emission (nm)	590	602	602	602	602
quantum yield[a]	$(1.0 \pm 0.1) \times 10^{-3}$	0.015 ± 0.003[a]	0.047 ± 0.005[a]	0.095 ± 0.005[a]	0.072 ± 0.011[a]
lifetimes (ns)		3.84 ± 0.12	3.87 ± 0.03	4.05 ± 0.04	3.97 ± 0.05
	0.173 ± 0.009	1.71 ± 0.01	1.56 ± 0.04	1.68 ± 0.17	1.68 ± 0.05
		0.173[b]	0.173[b]	0.173[b]	0.173[b]

[a] Calculated quantum yields represent average values, because there may be a mixture of different species depending on the experimental conditions. [b] Because the value of the shortest lifetime is close to the instrumental response, it was kept fixed for the fitting to the value experimentally obtained for free BOBO-3 in solution (in the absence of DNA).

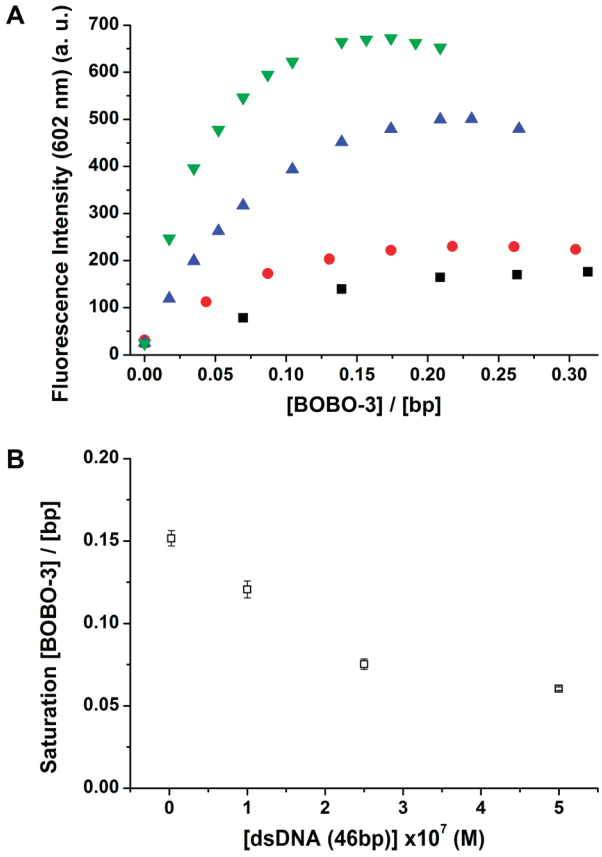

Figure 2. (A) Emission intensity at 602 nm ($\lambda_{ex} = 571$ nm) of BOBO-3 at different ratios dsDNA (46 bp) for different dsDNA concentrations: 5×10^{-7} M (green); 2.5×10^{-7} M (blue); 1×10^{-7} M (red); 2.5×10^{-8} M (black). (B) Dependence of saturation, as the number of base pairs per BOBO-3 molecule, with the total dsDNA (46 bp) concentration. Error bars represent standard deviations from at least three repetitions.

the weakness of expressing the number of sites covered by an intercalator dye through this approach, because it depends on the experimental conditions, making it evident that other treatments are required. These variations actually respond to the equilibrium theory, i.e., larger dsDNA concentrations promote further formation of complexes, and less BOBO-3 is required to reach saturation, therefore reaching the fluorescence intensity maximum at a lower BOBO-3/DNA bp ratio (Figure 2). This was further supported by the fact that once the saturations had been reached, the addition of more dsDNA caused further increase in the fluorescence emission, promoting the formation of more fluorescent complexes (Figure S2). Double-stranded DNA of shorter lengths showed the same behavior, confirming this was not an effect over short DNA strands (Figure S3).

Similar experiments were performed using single-stranded DNA (15 and 46 nucleotides) in order to test the interactions detected in the absorption spectra. When BOBO-3 was added to 46-nucleotide ssDNA, an enhancement of the emission intensity at 602 nm was detected, although not as significant as that observed with dsDNA. For instance, for a fixed [BOBO-3]/[base] ratio of 0.04, the enhancement of emission intensity for ssDNA (46 nucleotides) was 25-fold, and for dsDNA (46 bp) was 35-fold. However, negligible changes in emission spectra of BOBO-3 upon addition of 15-nucleotide ssDNA were observed. These results clearly indicate that BOBO-3 does not interact with 15-nucleotide ssDNA to form the enhanced fluorescent species, but another type of interaction does exist which cause variations in the absorption spectra. The spectral features of the complexes between BOBO-3 and ssDNA, along with the dsDNA experiments, are gathered in Table 1.

Melting Experiments. We performed melting experiments followed by absorption measurements in order to determine whether BOBO-3 intercalates into partially self-hybridized ssDNA that may or may not be induced by the dye itself, favoring intercalation. Absorption spectra of 46-nucleotide ssDNA (2.5×10^{-7} M) at different temperatures were recorded, in the presence and in the absence of excess of BOBO-3 (5×10^{-7} M). For that, the holders were thermostatically controlled between 20 and 100 °C. The absorption intensity at 260 nm did not change for ssDNA in the absence of BOBO-3 in the entire range of temperatures tested, nor did the absorption maximum shift (Supporting Information Figure S4). This suggests the absence of self-hybridization or interaction between single strands. However, in the presence of BOBO-3, hyperchromicity at 260 nm was observed over 60 °C. In addition, the absorption spectrum of BOBO-3 was gradually changing, observing the gradual shift to blue of the absorption maximum corresponding to BOBO-3 free in solution by increasing the temperature (Figure 3). After slow cooling, the absorption intensity returned to the original value and the shape of the absorption spectrum of BOBO-3 was shifted to the initial complexed form. Importantly, this effect was negligible for 15-nucleotide ssDNA. These results indicate that BOBO-3 favored self-hybridization of the strands and the concomitant intercalation of the dye. The additional stabilization of double-stranded DNA structures upon the addition of an intercalator has been previously detected for BOBO-3[20] and other dyes,[20−23] suggesting that the intercalation favors the annealing of partially complementary strands.

Time-Resolved Fluorescence Spectroscopy. Additional time-resolved fluorescence experiments were performed to further explore the temporal behavior of BOBO-3 emission. In the absence of DNA, the fluorescence decay profiles of free BOBO-3 in aqueous 10 mM Tris-HCl, 1 mM EDTA, and 100 mM NaCl pH 7.5 buffer were found to follow monoexponential functions. A 10^{-5} M BOBO-3 solution provided a lifetime of 0.173 ± 0.009 ns. This short lifetime agrees with the low quantum yield calculated for free BOBO-3 using Rhodamine B as reference (QY = 0.001).

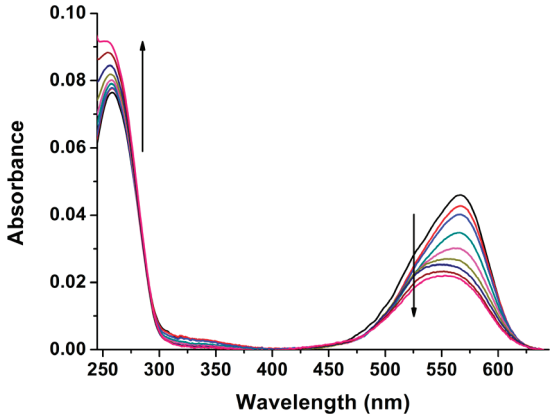

Figure 3. Absorption spectra of 46-nucleotide ssDNA (5×10^{-7} M) in the presence of BOBO-3 (5×10^{-7} M) at different temperatures: 20, 30, 40, 50, 60, 70, 80, 90, and 100 °C. Arrows indicate an increase in temperature.

In the presence of dsDNA, samples at different [BOBO-3]/[DNA bp] ratios were prepared, using 15 and 46 bp dsDNA, and fluorescence decay traces were recorded at 590, 600, 610, and 620 nm emission wavelengths. Similarly, we collected fluorescence decay traces of BOBO-3 in the presence of ssDNA of 15 and 46 nucleotides at different [BOBO-3]/[base] ratios. The four decay traces from each mixture at different emission wavelengths were fitted globally with the decay times linked as shared parameters, whereas the pre-exponential factors were local adjustable parameters. In all cases, the best fits required a sum of three exponential decay functions to reach low χ^2 values as well as random distributions of the weighted residuals and autocorrelation function, indicators of the goodness of the fits. Figure 4 shows an example of fluorescence decay traces of BOBO-3 free in solution and in the presence of single-stranded and double-stranded DNA of different lengths.

Table 1 shows the average values of the lifetimes for the different interactions of BOBO-3 with ssDNA and dsDNA. We also show in Table S2 in Supporting Information, as an example, the results of global fits for some dye/15 bp dsDNA mixtures, including the recovered decay times and pre-exponential factors. In each case, a short lifetime was detected, the value of which was kept fixed to that obtained for BOBO-3 in solution. This is justified because the lifetime value is close to our temporal resolution limit and therefore difficult to be fitted accurately. The other two decay times were around 1.6 and 4.0 ns in every case, with different weights depending on the experimental conditions (Table S2). The values of the lifetimes were reproducible independent of the [BOBO-3]/[DNA bp] ratio, even though their abundances were very different. For instance, for [BOBO-3]/[dsDNA (46 bp)] in the range of ratios between 1/250 and 1/1, the average lifetimes were $\tau_1 = 3.97 \pm 0.05$ ns and $\tau_2 = 1.68 \pm 0.05$ ns. The dye in the presence of 15 and 46 bp dsDNA showed similar contributions for each decay time under a large range of conditions, with the long time being the one with a higher weight (Figure 5). However, when a large excess of BOBO-3 is added, the short lifetime increased its contribution to the fluorescence. It is also important to note that the short lifetime always shows a higher contribution at the 590 nm emission wavelength than in the rest of the emission wavelengths collected. The short decay time does correspond to the free BOBO-3, and this species has its emission maximum at 590 nm, whereas the complexed dye shows a red-shifted emission maximum (Figure 1B). This is therefore in good agreement with the spectral features of the free dye in aqueous solution (short decay time with preferential emission at 590 nm).

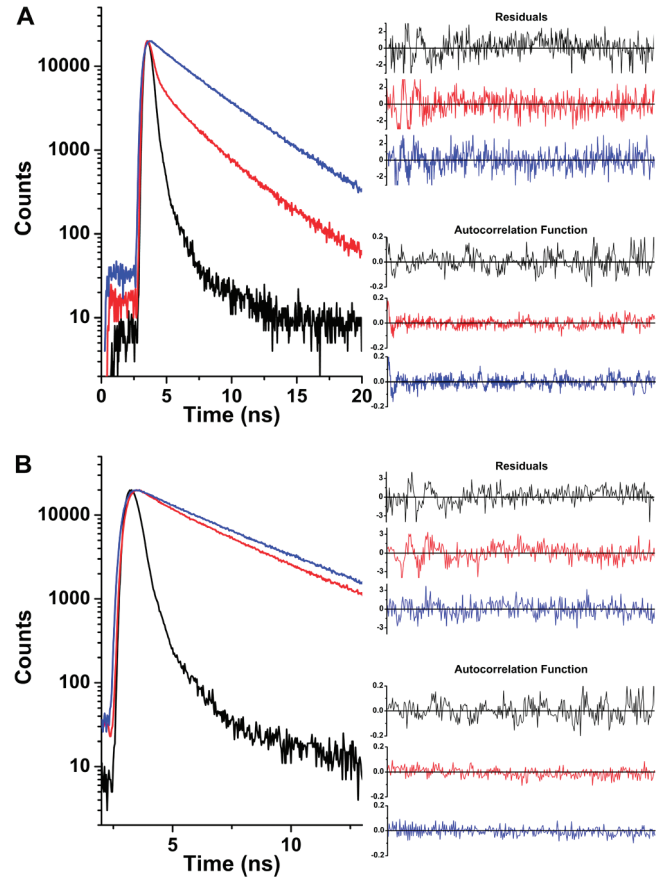

Figure 4. Fluorescence decay traces of BOBO-3/DNA mixtures (ratio 5:1): (A) BOBO-3 free in solution (black); BOBO-3/15 nucleotides-ssDNA (red); BOBO-3/dsDNA (15 bp) (blue). (B) BOBO-3 free in solution (black); BOBO-3/46-nucleotide-ssDNA (red); BOBO-3/dsDNA (46 bp) (blue). Excitation was by a 485-nm pulsed laser and emission collected at 600 nm. The residuals and autocorrelation functions from the triexponential fits are also shown.

Interestingly, BOBO-3 also showed triexponential fluorescence decay traces when interacting with ssDNA, with decay times similar to those recovered with dsDNA (Table 1). Importantly, the long decay time around 4.0 ns was only remarkable in 46-nucleotide ssDNA, whereas its contribution was almost negligible when 15-nucleotide strands were added. For 15-nucleotide ssDNA, the major component was thus the shortest decay time. The behavior was however similar to the one detected for dsDNA: the same spectral variance, with the short component giving rise to larger pre-exponential factors at 590 nm, and the increase in contribution of this shorter lifetime when a large excess of dye was added. The global analysis of fluorescence decay traces and the recovery of pre-exponential weights for each decay time allows back-calculation of the fraction of dye actually existing in each different microenvironment. This calculation has been described in Materials and Methods and basically consists of applying factors to the pre-exponentials that account for the differential excitation rates as well as the different contributions at each emission wavelength of the three species (Table S1 for these factors). By using these factors, we have obtained the fraction of BOBO-3 in each form (Figure 5): free in solution, corresponding to the shortest decay time; the partially quenched BOBO-3, corresponding to the intermediate lifetime; the amount of BOBO-3 with the longest decay time, intercalated into the DNA.

Expectedly, the pre-exponential factors of BOBO-3 in ssDNA were temperature-dependent. For instance, at 15 °C the normal-

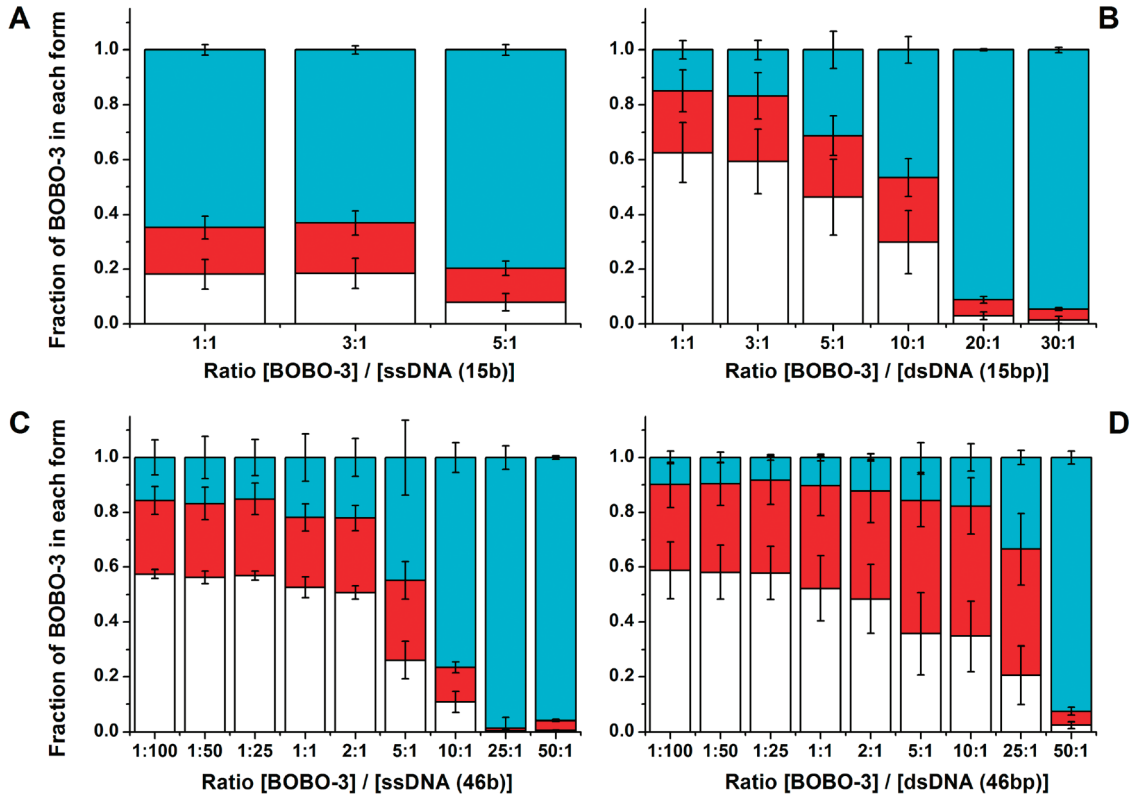

Figure 5. Mole fraction of BOBO-3 in each state, calculated from converted pre-exponential factors of τ_1 (long decay time, white), τ_2 (intermediate lifetime, red), and τ_3 (short decay time, cyan), under different BOBO-3/DNA ratios of single- or double-stranded DNA: (A) 15 nucleotides-ssDNA, (B) 15 bp dsDNA, (C) 46 nucleotides-ssDNA, and (D) 46 bp dsDNA. Error bars represent standard deviations from at least three repetitions.

ized pre-exponential calculated for τ_1, τ_2, and τ_3 were 0.52 ± 0.07, 0.28 ± 0.02, and 0.20 ± 0.09, for the longer, intermediate, and shorter lifetime, respectively. However, at 80 °C the normalized pre-exponential of the intermediate and short lifetime increased to 0.44 ± 0.13 and 0.25 ± 0.02, respectively (Figure S5).

In order to check the nature of the interactions giving rise to the intermediate lifetime, we finally tested the effect of ionic strength and electrostatic interactions on the three populations of BOBO-3 in dsDNA. Fluorescence decay profiles of [BOBO-3]/[dsDNA (46 bp)] at the same ratio (10:1) but at different ionic strengths were studied (Figure S6). At higher NaCl concentration the pre-exponential of τ_2, the intermediate lifetime, decrease slightly. The normalized pre-exponential of the intermediate lifetime varied from 0.27 ± 0.06 at 0.1 M NaCl to 0.12 ± 0.04 at 0.5 M NaCl, increasing the fraction of the short lifetime and keeping the contribution of the long lifetime.

Discussion

BOBO-3 Presents Two Binding Modes to ss- and ds-DNA. Analysis of all the results described above clearly indicates that the interaction between BOBO-3 dye and oligonucleotides cannot be explained with a simple, single intercalation mechanism. Moreover, it is a common feature of intercalating dyes to show different modes of interaction. To date, studies on cyanine dimer binding modes have been focused on YOYO-1 and TOTO-1 dyes. YOYO-1 was found to exhibit at least two distinct binding modes. At low dye/bp ratios, the binding mode appears to consist primarily of bis-intercalation.[6] Each monomer unit intercalates between bases, with the benzazolium ring system sandwiched between the pyrimidines and the quinolinium ring between the purine rings, causing the helix to unwind, but at high dye/bp ratios, a second, less well characterized mode of external binding begins to contribute.[5] TOTO-1 is also capable of bis-intercalation,[7] but an external binding mode, where the dipole of the dye molecule is aligned with the DNA grooves, may also be important.[9] Hence, BOBO-3 showed behavior similar to that of other members of the family. Here we have performed a thorough study of the interactions of BOBO-3, which provided additional information to better understand the nature of these interactions. To test the performance of the equilibrium theory involving a single binding mode of BOBO-3, we have applied the treatment developed by Yguerabide and Ceballos.[12] We analyzed the steady-state fluorescence emission behavior of BOBO-3 in the presence of dsDNA under different conditions: first, increasing concentrations of the intercalating dye at a constant dsDNA concentration, and second, once saturation is reached, the addition of more dsDNA. The single binding mode turned out to be insufficient to explain the emission features of BOBO-3 (see Supporting Information for the equations and Figure S7) and suggested the need for a more detailed model.

A close look at the absorption and fluorescence emission spectra of BOBO-3 in both dsDNA and ssDNA already suggests different modes of interaction. Indeed, BOBO-3 interacts strongly with ssDNA and dsDNA, undergoing a relaxation of the excited state, and a red-shift of the absorption maximum. However, BOBO-3 is only strongly fluorescent in dsDNA and much less in ssDNA. This supports that, although the interaction occurs, the fluorophore environment in either dsDNA or ssDNA is different. Furthermore, in ssDNA the length of the oligonucleotide showed differential effects on the BOBO-3 behavior. A longer nucleotide gave rise to slightly higher fluorescence intensity, and the melting experiments confirmed that this was due to BOBO-3 intercalating into self-hybridized strands induced by the dye. DNA single strands are able to form transient

contacts, such as regional stem-loops or hairpins, and these structures may be stabilized by the presence of a high affinity binding molecule.[24] This stabilizing effect has been previously described for other intercalator dyes that cause an increase in dsDNA melting temperature with increasing dye concentration.[25,26] This further stabilization when an intercalating dye is present has also been detected with cyanine derivatives. With YOYO and YO-PRO the melting temperature of the DNA was observed to increase in direct proportion to the number of occupied intercalation sites on the DNA.[23] Several effects can be considered to be responsible for the duplex stabilization, such as stacking interactions, screening of the DNA backbone's negative charges by the positively charged dye, and local structural modifications on the double helix that reduce charge density.

The inspection of the average quantum yields (Table 1) calculated under different experimental conditions supports the presence in the solution of at least two modes of interaction with DNA as well as the free, unbound dye. At low mixing ratios BOBO-3/dsDNA, practically all the dye present in solution is bound to the dsDNA intercalated into the DNA double helix, like other cyanine derivatives. This intercalating binding mode protects the dye for the solvent quenching and provides higher fluorescence quantum yield ($\sim$0.07$-$0.09). It is important to note that this quantum yield value is actually an average, or apparent, value because it includes all three species present in solution. However, this value is valid to proceed with direct comparisons, which would reveal variations in the relative populations of the species involved. For instance, increasing the BOBO-3/dsDNA ratio results in a slight blue shift of the absorption spectra along with a decrease in BOBO-3 apparent quantum yield (down to 0.01). This fact suggests that after saturation of the intercalating binding sites the excess BOBO-3 remains in solution, with a low quantum yield, or interacts with dsDNA in a less fluorescent mode.

Time-Resolved Fluorescence Allows Quantification of the Different Binding Modes. Nevertheless, the most convincing results that allow assignment of different binding modes were the time-resolved fluorescence measurements. In these, clearly three different environments of the fluorophore were observed (Table 1 and Table S2): a form with a lifetime τ_1 around 4.0 ns, a second species with τ_2 around 1.7 ns, and a highly quenched form (τ_3) that is unequivocally assigned to the unbound BOBO-3 in solution. These results are in agreement with the assumption that BOBO-3 binds to two different types of dsDNA binding sites. The first of these sites is the high-affinity intercalating site, where the dye is highly protected and shows a longer lifetime, whereas the second is a less fluorescent complex. The secondary site may arise from several types of interactions; for instance, the binding may be due to electrostatic interactions between the positive charge of BOBO-3 and the negative charge of the phosphate groups of DNA. Cyanine dyes such as thiazole orange head groups of TOTO have a strong tendency to stack in aqueous solution;[27] therefore, interactions that involve formation of stacked dye aggregates along the polymer backbone also could be considered. Other stacking interactions[28] proposed a partial intercalation model of cationic dye binding to DNA as an alternative to the classic intercalation model. This 'partial intercalation-like' mode has been hypothesized in other dimeric cyanine dyes such as TOTO.[8] Because BOBO-3 is a dimeric cyanine dye it may also have the possibility of incomplete intercalation, by binding only one of the two moieties, resulting in a partially quenched form.

The values of the decay times were rather invariable over a large range of experimental conditions (Table S2), meaning the dye environment does not appreciably change with the dye/DNA ratio. Only at high BOBO-3/dsDNA ratios was a decrease in the lifetimes of BOBO-3 observed. This gradual decrease is in agreement with the quenching of the steady-state fluorescence signal observed under similar conditions. This quenching is explained by the excess BOBO-3, saturating most of the available primary and secondary sites, which may cause self-quenching or nonradiative resonance energy transfer between the bound fluorophores. Other authors found a similar effect in EtBr but suggested energy transfer between intercalated dye and free fluorophore in solution.[29,30] However, it is not likely that the energy transfer occurs toward unbound, freely diffusing dye molecules that on average would be far away from the complexed dyes. In our study, the self-quenching is more likely to be due to energy transfer from intercalated dye in the primary sites toward the less fluorescent form in the secondary positions, because of their close proximity.

To gain more insight into the nature of the two binding modes, we have performed several time-resolved fluorescence measurements involving single- and double-stranded DNA of different lengths. The comparison between these four situations provided more evidence on the behavior of the two binding modes. Following the pre-exponential factors associated to each form of BOBO-3, it is possible to describe the behavior of the intercalators with the change in dye/DNA ratio. As it is known, relative emission amplitudes are proportional to the number of emitting species with the corresponding lifetime values. Here, we calculated the fraction of BOBO-3 participating in the different interactions from the values of pre-exponential factors obtained in the fitting. The calculation takes into account the differential excitation rates of the free dye versus the intercalated fluorophore at the laser excitation wavelength, as well as the different contributions at each emission wavelength of the three species, as described in Materials and Methods. The calculated mole fractions provided the contribution of each binding mode for all BOBO-3/dsDNA ratios. Some examples of BOBO-3 in the presence of different amounts of dsDNA of 15 and 46 base pair lengths are given in Figure 5. For a fixed dsDNA concentration (1×10^{-7} M), by increasing the quantity of BOBO-3 added, the fractions of the primary intercalation mode decreased gradually. In contrast, the relative contribution of the secondary sites initially increased slightly with BOBO-3 concentration, suggesting that although the primary sites are totally occupied, there may be some more available secondary sites. At much higher BOBO-3 concentrations, the contribution of the shortest lifetime increases drastically when all the sites are used, and the excess dye remains free in solution. Although at these conditions of high BOBO-3 levels the quenching of the fluorescent forms may be appreciable, as the decrease in the lifetimes indicates, it should not affect the relative amplitudes of the three emitting species. This behavior in general terms was followed indistinguishably in both 15 and 46 base pair duplexes (Table S2). The effect of BOBO-3 in ssDNA is also interesting. In general, the same three decay times were obtained in the fitting of fluorescence decay traces of BOBO-3 in the presence of ssDNA of 15 and 46 nucleotides, which suggests similar interaction modes (see Figure 5). However, clear differences arose between the different lengths of ssDNA. Within the 15-nucleotide single strand, BOBO-3 showed almost negligible contribution of the intercalated species, which suggests almost total absence of intercalation between the dye and the single strand. On the contrary, BOBO-3 in the presence of

46-nucleotide ssDNA showed an important contribution of both modes of interaction. This also agrees with the intrinsic emission at 602 nm of BOBO-3 after interaction with 46-nucleotide ssDNA and the relatively high apparent quantum yield calculated (Figure 1B and Table 1). As it occurs in dsDNA, by increasing the BOBO-3/ssDNA ratio, the fraction of BOBO-3 free in solution increased (see Figure 5), with a concomitant slight decrease of the fraction of intercalated BOBO-3 (even though the total amount of intercalated BOBO-3 remains constant). We believe that the presence of BOBO-3 facilitates self-hybridization of DNA strands because of an extra stabilization of the duplex, as reported for other cyanine dimeric dyes,[23] and we confirmed this by melting experiments with UV−vis spectroscopy (Figure 3 and Figure S3). This is additionally supported by the fluorescence decay traces at different temperatures (Figure S5). However, when increasing the temperature to 80 °C, the most favored form is that bound to secondary sites, leading us to conclude that the secondary sites do not require the formation of a duplex but rather direct interactions with either the bases or the negative charges of the phosphate backbone. The contrast between the short and long strand lies in the fact that self-hybridization is more likely to occur in longer ssDNA strands because of the higher chance to form more stable contacts. We then have tested the nature of the secondary binding sites by investigating the effect of the ionic strength. Assuming that the secondary interactions involve electrostatic attraction between the positively charged BOBO-3 and the DNA backbone, we studied the effect of increasing salt concentration that leads to a counterbalance of negative charges in the phosphate backbone. Increasing salt concentration in BOBO-3/dsDNA (46 bp) clearly reduced the contribution of the secondary sites (Figure S6), implicating the need for electrostatic attraction to facilitate binding to secondary sites. As expected, the fraction of BOBO-3 in the primary intercalation mode was maintained in all cases, and the decrease in the secondary binding mode was counteracted by the increase in the contribution of the free dye.

BOBO-3 Follows the McGhee−von Hippel Theory. Importantly, having a direct measurement of the fraction of each form of BOBO-3 provided the necessary information to further quantify the system by applying the McGhee−von Hippel theory.[11,13] This theory directly accounts for ligand interactions with linear distribution of binding sites. We analyzed our results according to McGhee−von Hippel theory considering two overlapping, noncooperative binding modes through the methodology described in Materials and Methods. This analysis allowed the recovery of binding constants for each binding mode, K_1 and K_2, and the number of sites (base pairs) covered for a dye molecule bound in each mode, n_1 and n_2. The global fit of the whole surface of experiments under different conditions using BOBO-3 and dsDNA of 46 base pairs provided accurate values for K_j and n_j, using the methodology described earlier. The concentrations of bound BOBO-3 in each binding mode under the different experimental conditions obtained via time-resolved fluorescence and pre-exponential factors analysis are shown in Figure 6A and 6B. These data were expressed in terms of r_1 and r_2 ($[\text{BOBO-3}]_{\text{mode\_1}}/[\text{DNA}_{\text{bp}}]$ and $[\text{BOBO-3}]_{\text{mode\_2}}/[\text{DNA}_{\text{bp}}]$, respectively), bound dye per base pair, versus the total concentration of BOBO-3 per base pair (r_{tot}). The simultaneous fit of the whole surface of the two modes provided the following results: for mode 1, or the complete bis-intercalation, the recovered binding constant was $(8.8 \pm 1.1) \times 10^5\ \text{M}^{-1}$, covering 5.9 ± 0.2 sites (base pairs); whereas for mode 2, the binding constant was $(2.6 \pm 0.3) \times 10^5\ \text{M}^{-1}$ and n_2 was 3.5 ± 0.5 sites. Figure 6C shows the whole fitted surface of r_1 and r_2 vs r_{tot} at six different total dsDNA concentrations, whereas Figure 6D shows the experimental points and the corresponding fitting curves. With these results we unequivocally assigned binding mode 1 to the bis-intercalation, because the dye covers up to six base pairs, in agreement with the structural arrangement suggested for other bis-intercalator cyanine dyes.[4,6,31] The obtained binding constant is remarkably lower than other values reported for cyanine homodimers that are about 3−6 orders of magnitude larger.[4] For instance, the reported binding constant value for TOTO dyes is approximately $10^9\ \text{M}^{-1}$,[3,32] and the binding constant for YOYO with dsDNA has been estimated to be in the range of $10^{10}-10^{12}\ \text{M}^{-1}$.[2,5] However, most of the previously reported values are rough estimations that do not take into account McGhee and Von Hippel's treatment and are usually performed with very long fragments of DNA far apart from the saturation point. Furthermore, the binding mechanisms of YOYO and TOTO dyes are likely to be of a different nature as indicated by a much slower DNA staining, in the range of hours, in contrast to BOBO or POPO which form DNA complexes within minutes.[7] In this work, at the concentrations employed, the affinity between the dye and the DNA is relatively low, which causes the ubiquitous presence of a certain amount of unbound, free BOBO-3 in solution. The use of a time-resolved fluorescence methodology, however, allowed detection of this fraction of free BOBO-3 and accurately quantitation of its contribution. Regarding the second mode of interaction, the most remarkable feature is that its binding affinity is of the same order as that of the main binding mode. This always causes a distribution of dye molecules between the two modes. The two binding modes are self-excluding, therefore affecting the fluorescent properties of the dye upon interaction with dsDNA. However, the presence of this kind of interaction also in single-stranded DNA (as shown in Figure 5A and 5C) and the effect of ionic strength on the interaction supports the idea of an electrostatically driven form of complexation, facilitated by charges of opposite sign in the BOBO-3 moiety and the DNA phosphate backbone. Moreover, the similar affinity of both modes results in poor selectivity of binding to dsDNA with respect to ssDNA, as it occurs for other dyes of the family, because the electrostatic interactions are equally effective in single or double strands. This is of high relevance to use these dyes in real-time PCR. Highly positively charged intercalators, BOBO-3 among them, have shown poor performance in PCR due to affinity to ssDNA, stabilization of transient structures, and effect on the melting temperature of the dsDNA.[20,24]

Conclusions

We have performed a thorough investigation of the photophysics and intercalation properties in small fragments of DNA of the homodimeric cyanine dye BOBO-3. As for other DNA intercalator fluorophores, the main photophysical feature of the dye is an extensive enhancement of the fluorescence emission upon intercalation into dsDNA. The fluorescence emission enhancement is related to the prevention of the rotation between the two chromophore groups, decreasing nonradiative relaxations. However, the interaction of BOBO-3 with DNA is not only reduced to a simple intercalation mode. Indeed, we have shown BOBO-3 forms complexes with single-stranded DNA in a different binding mode that also modifies the spectral properties of the dye, making BOBO-3 a poor probe for DNA hybridization. The low affinity binding mode is likely to be driven by electrostatic interactions, because the dye is positively charged, but the change in spectral properties suggests a partial hybridization of the fluorophore. This binding mode coexists

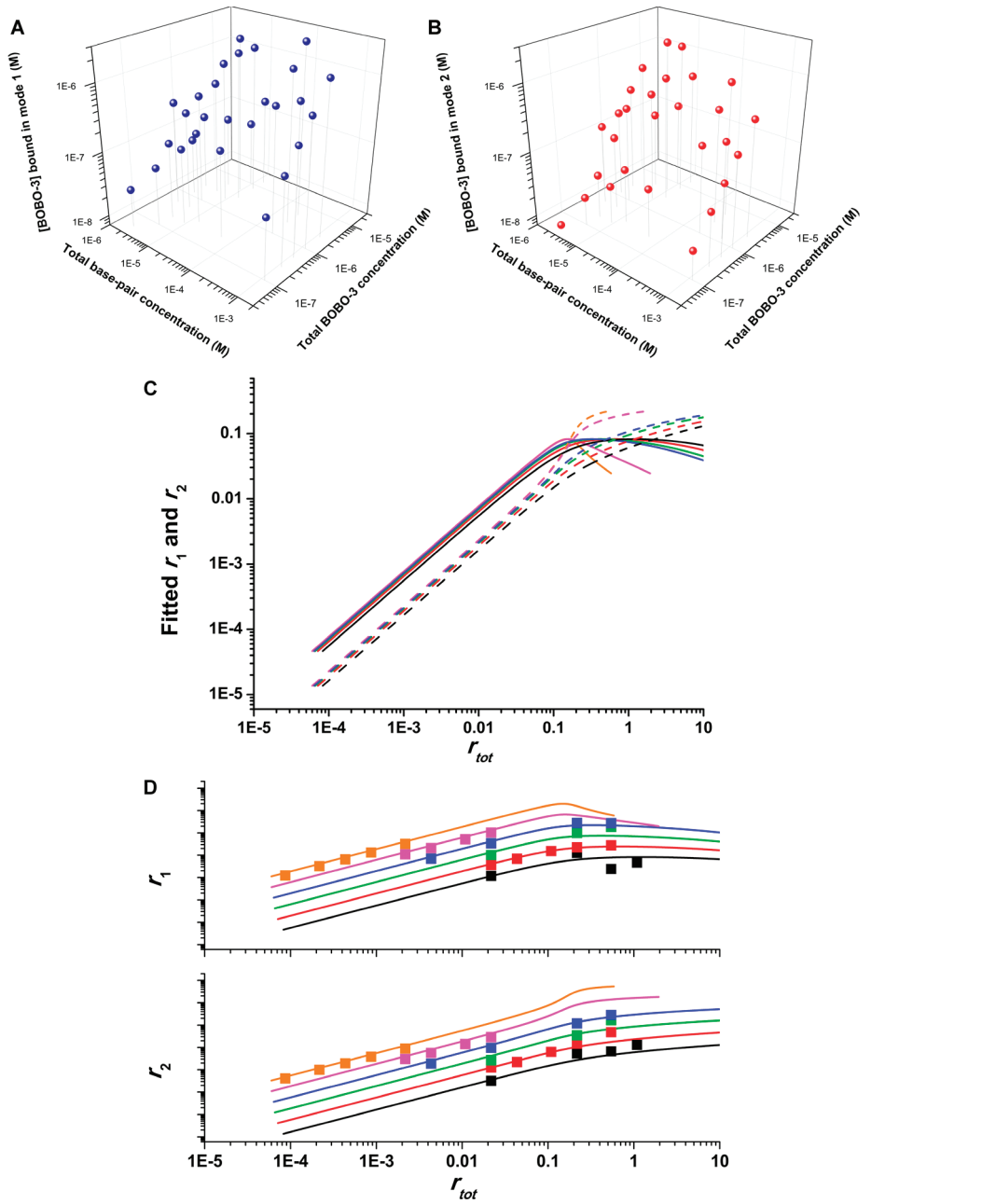

Figure 6. Concentration of bound BOBO-3 in (A) mode 1 (complete bis-intercalation) and (B) mode 2 (electrostatically driven interactions) at different total 46 bp dsDNA and total BOBO-3 concentrations. (C) Fitted curves of bound BOBO-3 per base pair in mode 1 (solid lines, r_1) and mode 2 (dashed lines, r_2) versus total concentration of BOBO-3 per base pair (r_{tot}), at different total dsDNA concentrations: 5×10^{-8} (black), 1.0×10^{-7} (red), 2.0×10^{-7} (green), 3.0×10^{-7} (blue), 5.0×10^{-6} (magenta), and 2.5×10^{-5} M (orange). (D) Experimental points and calculated curves of bound BOBO-3 per base pair in mode 1 (r_1) and mode 2 (r_2) versus total concentration of BOBO-3 per base pair (r_{tot}) presented with a constant shift for better visualization, and following the same color code as that in C. Error bars lay within the symbols.

and competes with a clamp-like bis-intercalation mechanism. In this work, we have developed a time-resolved fluorescence methodology to quantify the contributions of BOBO-3 interacting with DNA in each binding mode. This allowed us to directly assess the affinity equilibrium constants and the number of sites (base pairs) covered by each BOBO-3 binding mode, according to the McGhee−Von Hippel theory of two overlapping, noncooperative binding modes. In the presence of dsDNA, the dye is distributed between the two competing modes and the free state in solution, according to very similar affinity constants. It is noteworthy that the low affinity mode covers around half the base pairs as that of the bis-intercalation, supporting the idea of a partial intercalation. A schematic of BOBO-3 behavior, spectral features, and binding constants, according to our findings, is shown in Figure S8. In summary, we presented here a comprehensive study of the fluorescence features of DNA intercalators BOBO-3, setting up the basis for a better understanding of fluorescence results when the dye is used, for example, in DNA hybridization detection or PCR amplification probes.

Acknowledgment. This work was supported by grants CTQ2007-61619/BQU from the Ministerio Español de Educación y Ciencia (cofinanced by the Fondo Europeo de Desarrollo Regional, FEDER), and P07-FQM-3091 from the Consejería de Innovación, Ciencia y Empresa (Junta de Andalucía). A.O. acknowledges an ERG contract from the seventh EU Framework.

Supporting Information Available: Detailed description of the methods, supporting text, Tables S1 and S2, and Figures S1−S8 are available free of charge via the Internet at http://pubs.acs.org.

References and Notes

(1) Glazer, A. N.; Peck, K.; Mathies, R. A. *Proc. Natl. Acad. Sci. U.S.A.* **1990**, *87*, 3851–3855.

(2) Glazer, A. N.; Rye, H. S. *Nature* **1992**, *359*, 859–861.

(3) Rye, H. S.; Yue, S.; Wemmer, D. E.; Quesada, M. A.; Haugland, R. P.; Mathies, R. A.; Glazer, A. N. *Nucleic Acids Res.* **1992**, *20*, 2803–2812.

(4) Haugland, R. P. *Handbook of Fluorescent Probes and Research Products*; Molecular Probes, Inc.: Eugene, OR, 2002.

(5) Larsson, A.; Carlsson, C.; Jonsson, M.; Albinsson, B. *J. Am. Chem. Soc.* **1994**, *116*, 8459–8465.

(6) Johansen, F.; Jacobsen, J. P. *J. Biomol. Struct. Dyn.* **1998**, *16*, 205–222.

(7) Carlsson, C.; Jonsson, M.; Akerman, B. *Nucleic Acids Res.* **1995**, *23*, 2413–2420.

(8) Rye, H. S.; Glazer, A. N. *Nucleic Acids Res.* **1995**, *23*, 1215–1222.

(9) Schins, J. M.; Agronskaia, A.; de Grooth, B. G.; Greve, J. *Cytometry* **1999**, *37*, 230–237.

(10) Talavera, E. M.; Bermejo, R.; Crovetto, L.; Orte, A.; Alvarez-Pez, J. M. *Appl. Spectrosc.* **2003**, *57*, 208–215.

(11) McGhee, J. D.; von Hippel, P. *J. Mol. Biol.* **1974**, *86*, 469–489.

(12) Yguerabide, J.; Ceballos, A. *Anal. Biochem.* **1995**, *228*, 208–220.

(13) Gaugain, B.; Barbet, J.; Capelle, N.; Roques, B. P.; Le Pecq, J. B. *Biochemistry* **1978**, *17*, 5078–5088.

(14) Byrne, C. D.; de Mello, A. J. *Biophys. Chem.* **1998**, *70*, 173–184.

(15) Hernandez, L. I.; Zhong, M.; Courtney, S. H.; Marky, L. A.; Kallenbach, N. R. *Biochemistry* **2002**, *33* (44), 13140–13146.

(16) Yguerabide, J.; Yguerabide, E., Nanosecond Fluorescence Spectroscopy. In *Optical Techniques in Biological Research*; Rousseau, D. L., Ed.; Academic Press: New York, 1984.

(17) Talavera, E. M.; Guerrero, P.; Ocana, F.; Alvarez-Pez, J. M. *Appl. Spectrosc.* **2002**, *56*, 362–369.

(18) Cosa, G.; Focsaneanu, K.-S.; Scaiano, J. C.; McLean, J. R. N. *Chem. Commun.* **2000**, 689–690.

(19) Magde, D.; Rojas, G. E.; Seybold, P. G. *Photochem. Photobiol.* **1999**, *70* (5), 737–744.

(20) Gudnason, H.; Dufva, M.; Bang, D. D.; Wolff, A. *Nucleic Acids Res.* **2007**, *35* (19), e127.

(21) Lepecq, J. B.; Paoletti, C. *J. Mol. Biol.* **1967**, *27* (1), 87–106.

(22) Douthart, R. J.; Burnett, J. P.; Beasley, F. W.; Frank, B. H. *Biochemistry* **1973**, *12* (2), 214–220.

(23) Bjorndal, M. T.; Fygenson, D. K. *Biopolymers* **2002**, *65* (1), 40–44.

(24) Mao, F.; Leung, W.-Y.; Xin, X. *BMC Biotechnol.* **2007**, *7* (1), 76.

(25) Ririe, K. M.; Rasmussen, R. P.; Wittwer, C. T. *Anal. Biochem.* **1997**, *245* (2), 154–160.

(26) Monis, P. T.; Giglio, S.; Saint, C. P. *Anal. Biochem.* **2005**, *340* (1), 24–34.

(27) Tyutyulkov, N.; Fabian, J.; Mehlhom, A.; Dietz, F.; Tadjer, A. Molecular and aggregate structures of polymethines. In *Polymethine Dyes. Structure and Properties*; St. Kliment Ohridski University Press: Sofia, 1991; pp 89−121.

(28) Pritchard, N. J.; Blake, A.; Peacocke, A. R. *Nature* **1966**, *212* (5068), 1360–1361.

(29) Burns, V. W. *Arch. Biochem. Biophys.* **1969**, *133*, 420–424.

(30) Heller, D. P.; Greenstock, C. L. *Biophys. Chem.* **1994**, *50*, 305–312.

(31) Spielmann, H. P.; Wemmer, D. E.; Jacobsen, J. P. *Biochemistry* **2002**, *34* (27), 8542–8553.

(32) Mecklenburg, M.; Grauers, A.; Jönsson, B. R.; Weber, A.; Danielsson, B. *Anal. Chim. Acta* **1997**, *347*, 79–86.

JP909863C